SPECTRAL ANALYSIS OF ELASTIC WAVES SCATTERED BY OBJECTS WITH SMOOTH SURFACES

Y. H. Pao and V. Varadan
Cornell University
Ithaca, NY 14853

ABSTRACT

This is a summary of the research on NDE performed during the last two years by the authors and Professor W. Sachse and Messrs. S. Sancar and G. C. C. Ku of the Department of Theoretical and Applied Mechanics at Cornell University. The report is divided into three parts: (1) Theoretical Spectra - Results based on the method of wave function expansion and the method of transition matrix (T-matrix) will be presented for the scattering by a circular cylindrical, elliptic cylindrical, spherical, and spheroidal (prolate or oblate) inclusions in solids. Additional results for the scattering by two circular cylindrical inclusions will also be shown. (2) Interpretation of Spectra - Spectra of a fluid inclusion may be interpreted on the basis of the theory of normal modes, and those of a cavity from the principle of interference. Spectra for two cylindrical cavities exhibit new features which are related to the interferences of waves diffracted by each cavity. (3) Comparison with Experiments - Some of the theoretical spectra are compared with experimental results obtained by Professor W. Sachse and his associates.

Introduction

As discussed in Ref. 1, the spectrum of the pulses scattered by an obstacle in an elastic solid equals the product of the spectrum of the incident pulse and the spectrum of responses of the obstacle when it is excited by monochromatic waves. In an experiment, the spectrum of the incident pulse can be isolated from the total spectrum; hence, we consider only the spectrum generated by the obstacle when radiated with monochromatic waves.

Let $\underset{\sim}{u}^i(\underset{\sim}{x},\omega)\exp(-i\omega t)$ be the displacement vector due to the incident harmonic waves of angular frequency ω, and $\underset{\sim}{u}(\underset{\sim}{x},\omega)\exp(-i\omega t)$ be the total wave field in the medium at the location x. The amplitude of the scattered waves can be expressed as

$$\underset{\sim}{u}^s(\underset{\sim}{x},\omega) = \underset{\sim}{u}(\underset{\sim}{x},\omega) - \underset{\sim}{u}^i(\underset{\sim}{x},\omega) \tag{1}$$

Our aim is to determine $\underset{\sim}{u}^s(\underset{\sim}{x},\omega)$ as a function of $\underset{\sim}{x}$ and ω. From $\underset{\sim}{u}^s$, all other quantities of interest like stresses, velocities and scattering cross-sections can be easily calculated.

Theoretical Spectra

The method which we developed to determine $\underset{\sim}{u}^s(\underset{\sim}{x},\omega)$ is an extension of the transition matrix (T-matrix) method originally developed by P. C. Waterman[2] for acoustic waves (scalar waves). Based on Huygens' principle for waves in an elastic solid, the waves scattered by a body with surface S are related to the secondary sources at S and the primary source by the following integral formula[3]

$$\underset{\sim}{u}^i(\underset{\sim}{x}) + \int_S [\underset{\sim}{u}(\underset{\sim}{x}')\cdot\underset{\sim}{n}'\cdot\underset{\approx}{\Sigma}(\underset{\sim}{x}|\underset{\sim}{x}') - \underset{\sim}{t}(\underset{\sim}{x}')\cdot\underset{\approx}{G}(\underset{\sim}{x}|\underset{\sim}{x}')]dS' \tag{2}$$

$$= \begin{cases} \underset{\sim}{u}(\underset{\sim}{x}); & \underset{\sim}{x} \text{ outside S} \\ 0; & \underset{\sim}{x} \text{ inside S} \end{cases}$$

In the above formula, $\underset{\sim}{u}(\underset{\sim}{x}')$ and $\underset{\sim}{t}(\underset{\sim}{x}')$ are respectively the unknown displacement and traction vectors at $\underset{\sim}{x}'$, a point on S; $\underset{\sim}{n}'$ is the unit outward normal to S at $\underset{\sim}{x}'$ (Fig. 1). The functions $\underset{\approx}{G}$ and $\underset{\approx}{\Sigma}$ are respectively the Green's displacement tensor and the Green's stress tensor.

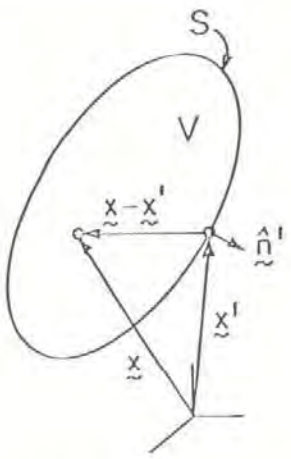

Figure 1. Mathematical model.

The essence of the transition matrix method is as follows: Select a set of vector basis functions $\phi_m^\sigma(x)$, $\psi_m^\sigma(x)$, and $\chi_m^\sigma(x)$ for vector waves in an elastic solid and then expand the unknown field $u^s(x)$ into a series of these basis functions.

$$u^s(x) = \sum_m \sum_{\sigma=1}^{2} [\alpha_m^\sigma \phi_m^\sigma(x) + \beta_m^\sigma \psi_m(x) + \gamma_m^\sigma \chi_m(x)] \quad (3)$$

The known incident field can be expanded into a series of the real parts of the basis functions denoted by $\hat{\phi}$, $\hat{\psi}$, $\hat{\chi}$,

$$u^i(x) = \sum_m \sum_\sigma [A_m^\sigma \hat{\phi}_m^\sigma(x) + B_m^\sigma \hat{\psi}_m^\sigma(x) + C_m^\sigma \hat{\chi}_m^\sigma(x)] \quad (4)$$

Since u^i is known, the coefficients A_m^σ, B_m^σ, and C_m^σ can be determined exactly. Substituting (3) and (4) into (2), we have shown that the unknown coefficients α, β, γ are related to A, B, C by an infinite matrix, known as the T-matrix[4].

$$\begin{pmatrix} \alpha_m^\sigma \\ \beta_m^\sigma \\ \gamma_m^\sigma \end{pmatrix} = \begin{pmatrix} T^{11} & T^{12} & T^{13} \\ T^{21} & T^{22} & T^{23} \\ T^{31} & T^{32} & T^{33} \end{pmatrix}_{mn}^{\sigma\nu} \begin{pmatrix} A_n^\nu \\ B_n^\nu \\ C_n^\nu \end{pmatrix} \quad (5)$$

Each element $(T^{ij})_{mn}^{\sigma\nu}$ represents an infinite sub matrix which depends on the choice of the basis function and the geometry of the bounding surface S. For a circular cylinder or a sphere, using circular cylindrical wave functions or spherical wave functions respectively, the T^{ij} can be determined exactly. For a body with a smooth, convex bounding surface, T^{ij} are determined from the surface integrals of the basis functions over S.

We note that P. C. Waterman[5] has given a matrix formulation for elastic waves beginning with a different integral representation.

Based on our formulation and a computer code developed by us, we can calculate $u^s(x,\omega)$ for a wide range of frequencies. Sample results are shown below (unless noted otherwise, inclusions are embedded in aluminum blocks):

(A)

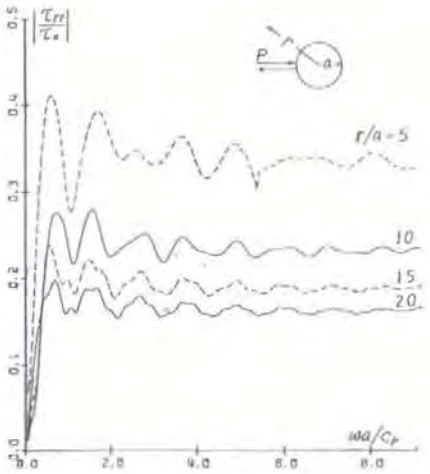

Figure 2. Backscattering of P-waves (longitudinal waves) by a circular cylindrical cavity (τ_{rr} is the radial stress, c_p the P-wave speed in solid).

(B)

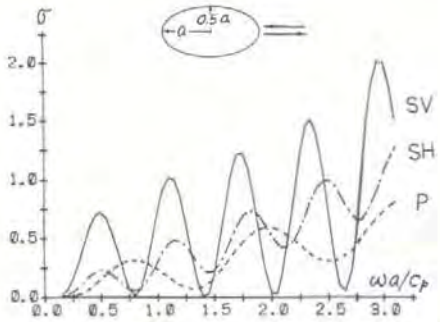

Figure 3. Backscattering by an elliptic cylindrical cavity for an incident P,SV (transversely polarized shear) and SH (horizontally polarized shear) wave along the major axis ($\bar{\sigma}$ is the differential cross section).

(C)

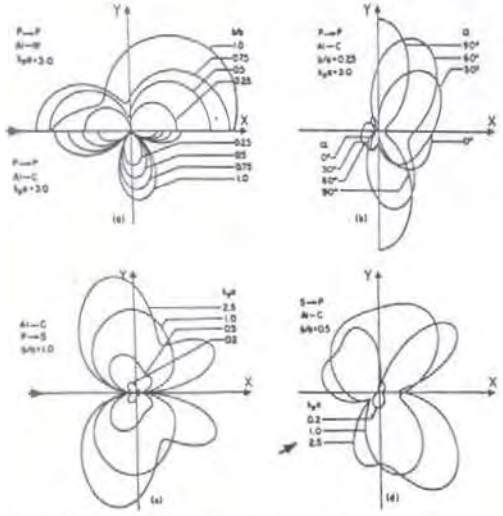

Figure 4. Angular distribution of far field scattered wave amplitudes by an elliptical cylinder with major axis 2a (along x-axis) and minor axis 2b. (Al-W indicates tungsten cylinder in aluminum matrix; Al-C indicates a cavity in aluminum solid; α the incident angle with respect to the x-axis)[7].

(D)

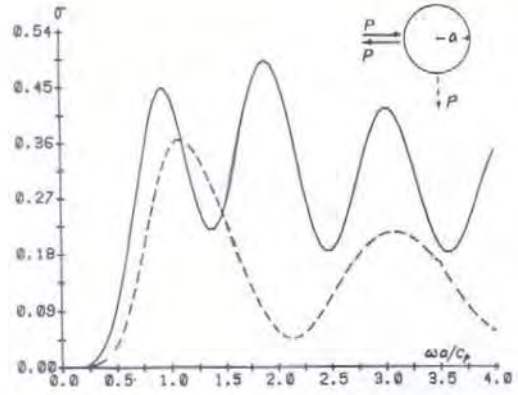

Figure 5. Backscattering and right-angle scattering of P-waves by a spherical cavity of radius 'a' (σ is the differential cross section)[8].

(E)

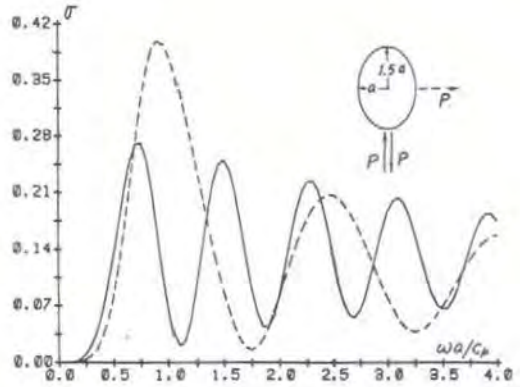

Figure 6. Backscattering and right-angle scattering of P-waves by a prolate spheroid (σ is the differential cross section)[9].

(F)

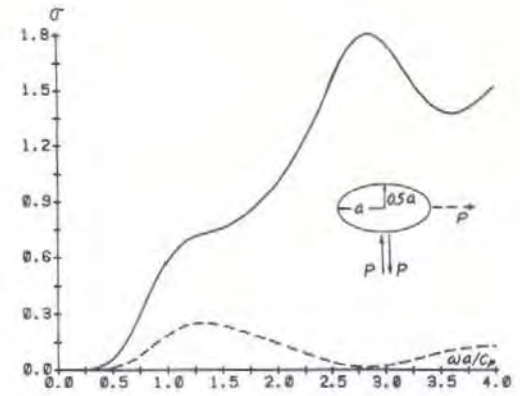

Figure 7. Backscattering and right-ang e scattering of P-waves by an oblate spheroid (σ is the differential cross section)[9]

(G)

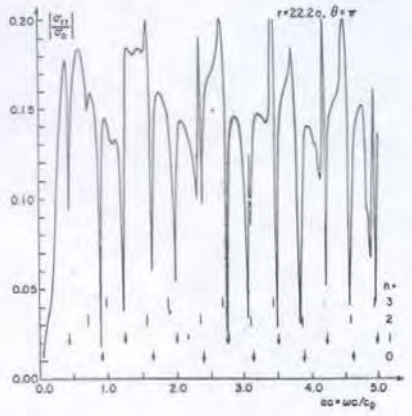

Figure 8. Backscattering of P-waves by a circular cylindrical cavity filled with water (τ_{rr} is the radial stress at distance r = 22.2a)[1].

In addition, we have made exact and approximate analysis of the multiple scattering of incident P-waves by two cylindrical cavities (Fig. 9) and two fluid cylinders (Fig. 10). The exact analysis is based on either the interactive method for multiple scattering developed by V. Twersky[11,12] or the T-matrix method for multiple scattering

(H)

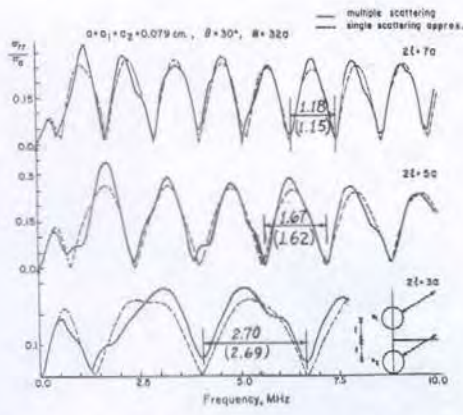

Figure 9. Backscattering of P-waves by two circular cylindrical cavities separated by a distance 2b, incident at an angle θ = 30° with the horizontal axis (σ_{rr} is the radial stress at distance R = 32a from the mid-point of two circles)[13]

(I)

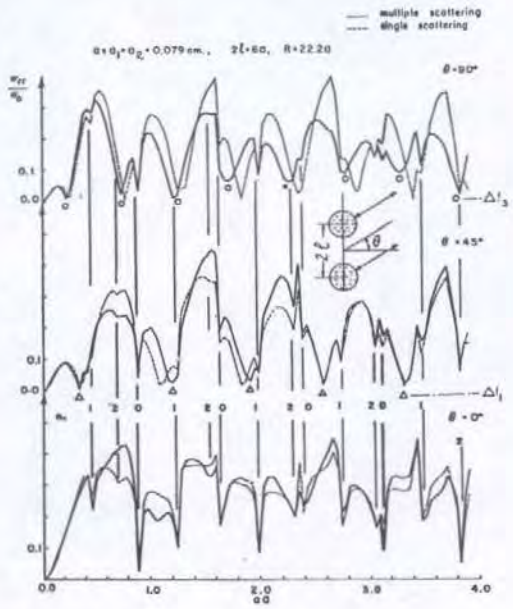

Figure 10. Backscattering of P-waves by two circular water cylinders at various angles of incidence (σ_{rr} is the radial stress, $\alpha a = \omega a/c_p$)[13].

Interpretation of the Spectra

We observe two features from these theoretical spectra: (1) all spectra of waves scattered by one or two cavities exhibit an obvious periodic structure; (2) the spectra of waves scattered by a liquid inclusion exhibits sharp peak and valley structure, which are quite different from those of a cavity. It is important to understand these features in order to apply spectral analysis to non-destructive evaluation of materials.

The periodicity of the spectra of a cavity may be understood from the interference of two rays of the scattered waves[6]. By a ray we mean the pulse propagating along a certain ray path connecting the receiver and the transmitter. Figure 11 shows an elliptical cavity and two ray-paths for backscattering. One is the direct reflected ray from the illuminated side of the cavity (PP or SS ray), the other is the creeping ray which runs around the shadow side of the cavity and then reaches the receiver (PP*P or SS*S ray).

Figure 11. Elliptical cavity and two ray-paths for backscattering.

The phase difference between these two rays is due to the different path lengths which is given by

$$\Delta(\text{Phase}) = 2a + 2aE(\tfrac{\pi}{2}, \varepsilon) \qquad (6)$$

where $\varepsilon = \sqrt{(1-b^2/a^2)}$ is the eccentricity of the ellipse and $E(\frac{\pi}{2}, \varepsilon)$ is the complete elliptic integral of the second kind. Because of the interference of waves traveling along these two paths, the spectra exhibit periodic structures. For PP and PP*P rays the period along the αa-axis ($\alpha = \omega a/c_p$) is

$$\text{P-wave:}\quad \Delta_p\,(\alpha a) = 2\pi/[\,2+2E(\tfrac{\pi}{2}, \varepsilon)] \qquad (7)$$

For SS and SS*S rays, we have

$$\text{S-wave:}\quad \Delta_S\,(\alpha a) = (c_S/c_p)\Delta_p(\alpha a)\ . \qquad (8)$$

Shown in Fig. 12 are three spectra of differential cross sections for the scattering of an incident SV, SH, and P-wave by an elliptical cavity in an aluminum solid. The spectra are the same as those shown in Fig. 3. On each graph, we measure the averaged periods in αa, which are marked above the dimension line. For the incident P-wave, we also calculated $\Delta_p(\alpha a)$ according to (7), which equals 1.428 and is marked below the dimension line inside parentheses. For the incident SV or SH wave, $\Delta_S(\alpha a) = 0.672$. We note that the agreement for the SH wave is very good, and the discrepancy for the SV and P-wave are not very large.

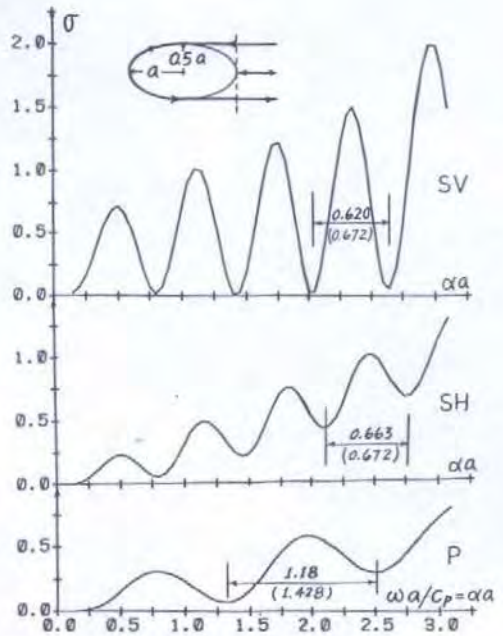

Figure 12. Spectra of differential cross sections for the scattering of an incident SV, SH, and P-wave by an elliptical cavity in an aluminum solid.

We also applied (6) to check the periods of spectra shown in Figs. 2, 3, and 5, 6. The agreement is always within 15 percent. The periods of the spectra for an oblate spheroid in Fig. 7 cannot be clearly determined.

On Fig. 9 we have indicated the periods 1.18, 1.67, and 2.70 (along frequency axis) of the spectra as measured from the thenetical spectra. In this case the periodicity is due to the interference of two rays reflected from each cylinder. The phase difference in length of these two rays is

$$\Delta(\text{Phase}) = 2(2\ell\sin\theta) \qquad (9)$$

Thus, along the frequency axis in Fig. .9, we expect to have a period of Δf,

$$\Delta f = c_p/(4\ell\sin\theta) \qquad (10)$$

The calculated values for Δf, 1.15, 1.62, and 2.69 are also shown in Fig. 9.

Since in all NDE work, we know in advance the values for c_p or c_s, knowing the periodicity of the spectra enables one to calculate the half-circumference of a cavity (Eqs. 7, 8) or the spacing between two cavities (Eq. 10).

For a cavity filled with fluid, the scattered spectrum is strongly affected by the natural frequencies of the fluid cylinder. The four lowest normal modes of a circular cylinder are shown in Fig. 13.[1] Each mode has a family of overtones (modes with additional modal circles). The natural frequencies of these modes and overtones can be calculated precisely, and the locations of the valleys of the backscattered spectra are formed to coincide with the overtone frequencies of modes n = 0 and n = 1. This has been thoroughly discussed in Ref. 1.

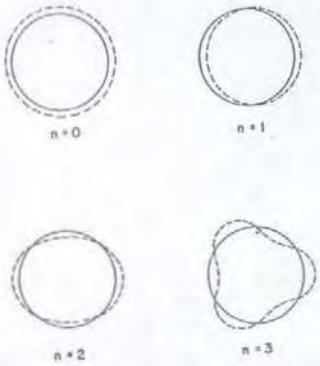

Figure 13. Four Lowest normal modes of a circular cylinder.

This theory of normal modes has been applied to interpret the spectra of the the scattering by two circular fluid cylinders. On Fig. 8 and 10, we show also the theoretical natural frequencies (in αa) for overtones of normal modes n = 0, 1 and 2. The four overtones of the zeroth mode (labeled with 0) and five overtones of the first mode (labeled with 1) all coincide with the valleys of all three spectra[1].

Since the natural frequencies depend on the radius of the cylinder and the speed of elastic waves in the fluid filling the cylinder it is possible to determine either from the detailed knowledge of the spectra.

Comparison with Experiments

Finally, we show a comparison between the theoretical spectra and the measured ones. In Fig. 14 are two measured spectra for the scattering of P-waves by a fluid cylinder in an aluminum block. Because the measured spectra include the spectra of the transducer, the magnitudes cannot be compared directly with the theoretical ones. However, the locations of the valleys (minima) coincide with the theoretical natural frequencies[14].

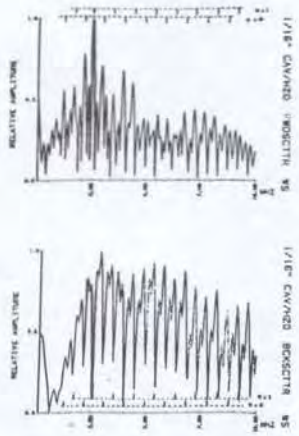

Figure 14. Comparison between the theoretical spectra and the measured ones.

On Fig. 15, we show both theoretical and experimental spectra of a P-wave scattered by two circular cavities in aluminum[13]. The spectrum of the incident pulse has been pre-determined and is divided from the scattered wave spectra. The agreement in the overall shape and the locations of maxima and minima is strikingly close.

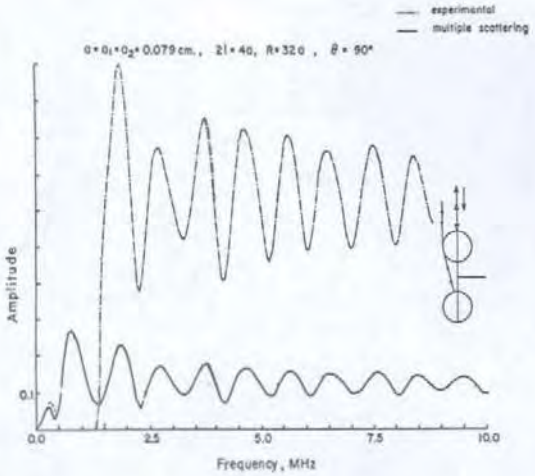

Figure 15. Theoretical and experimental spectra of a P-wave scattered by two circular cavities in aluminum.

In conclusion, we have shown that the transition matrix (T-matrix) method is very effective in calculating the theoretical spectra for waves scattered by an obstacle with smooth boundaries. The intricate structure of the spectra can be interpreted either by applying the principle of interference of two scattered rays, or from the theory of normal modes. Some of the theoretical spectra agree closely with experimentally determined ones.

Acknowledgement

This research was sponsored by the National Science Foundation (Grant No. ENG 75-13703) and the Material Science Center at Cornell University.

References

1. Y. H. Pao and C. C. Mow, J. Acoust. Soc. Am. 59, 1046 (1976).

2. P. C. Waterman, J. Acoust. Soc. Am. 45, 1417 (1969).

3. Y. H. Pao and V. Varatharajulu (V. V. Varadan), J. Acoust. Soc. Am. 59, 1361 (1976).

4. V. Varatharajulu (V. V. Varadan) and Y. H. Pao, J. Acoust. Soc. Am. 60, 556 (1976).

5. P. C. Waterman, J. Acoust. Soc. Am. 60, 567 (1976).

6. Y. H. Pao (to be published).

7. V. V. Varadan (to be published).

8. G.C.C. Ku, M.S. Thesis, Department of Theoretical and Applied Mechanics, Cornell University (1977).

9. V. V. Varadan (to be published).

10. V. Twersky, J. Acoust. Soc. Am. 24, 4245 (1952).

11. B. Peterson and S. Strom, J. Acoust. Soc. Am. 56, 771 (1952).

12. V. K. Varadan, V. V. Varadan and Y. H. Pao (to be published).

13. S. Sancar, Ph.D. Thesis, Department of Theoretical and Applied Mechanics, Cornell University (1977).

14. W. Sachse, F. Bifulco and Y. H. Pao, Material Science Report No: 2548, Cornell University (1975).